Neilson Bethany, T. (Orcid ID: 0000-0001-8829-5082)
Cardenas M. Bayani (Orcid ID: 0000-0001-6270-3105)
O'Connor Michael, Thomas (Orcid ID: 0000-0003-3484-4415)
King Tyler, Victor (Orcid ID: 0000-0002-5785-3077)
Kling George, W. (Orcid ID: 0000-0002-6349-8227)

Groundwater flow and exchange across the land surface explain carbon export patterns in continuous permafrost watersheds

Bethany T. Neilson[1*], M. Bayani Cardenas[2], Michael T. O'Connor[2],
Mitchell T. Rasmussen[1], Tyler V. King[1], and George W. Kling[3]

[1]Civil and Environmental Engineering, Utah Water Research Laboratory, Utah State University, Logan, UT 84322, USA. [2]Department of Geological Sciences, Jackson School of Geosciences, The University of Austin at Texas, Austin, TX 78712, USA. [3]Department of Ecology and Evolutionary Biology, University of Michigan, Ann Arbor, MI 48109, USA.

*Correspondence to: bethany.neilson@usu.edu.

Abstract

Groundwater flow regimes in the seasonally-thawed soils in areas of continuous permafrost are relatively unknown despite their potential role in delivering water, carbon, and nutrients to streams. Using numerical groundwater flow models informed by observations from a headwater catchment in arctic Alaska, USA, we identify several mechanisms that result in substantial surface-subsurface water exchanges across the land surface during downslope movement and create a primary control on dissolved organic carbon (DOC) loading to streams and rivers. The models indicate that surface water flowing downslope has a substantial groundwater component due to rapid surface-subsurface exchanges across a range of hydrologic states, from unsaturated to flooded. Field-based measurements corroborate the high groundwater contributions, and river DOC concentrations are similar to that of groundwater across large discharge ranges. The persistence of these groundwater contributions in arctic watersheds will influence carbon export to rivers if thaw depth increases in a warmer climate.

This is the author manuscript accepted for publication and has undergone full peer review but has not been through the copyediting, typesetting, pagination and proofreading process, which may lead to differences between this version and the Version of Record. Please cite this article as doi: 10.1029/2018GL078140

1. Introduction

Despite the importance of carbon (C) transport and fate in ecosystem function and greenhouse-gas driven climate change, there is still limited understanding of the hydrologic mechanisms controlling C transport from the landscape to surface waters [e.g., *Alexander et al.*, 2007; *Creed et al.*, 2015]. Water and solutes are delivered from groundwater to streams during dry periods, but overland flow can dominate during periods of rain or snowmelt. While the relative importance of groundwater versus overland flow on water and solute export depends on climate and catchment characteristics [*Jencso et al.*, 2009; *Wagener et al.*, 2007], there are expected patterns in solute delivery to streams in temperate-zone systems. For example, precipitation often increases concentrations of dissolved organic carbon (DOC) due to flushing of older water from soils, especially in headwater streams [*McGlynn and McDonnell*, 2003], while larger rivers are more chemostatic, where concentrations are similar over broad discharge ranges [*Creed et al.*, 2015].

Transport of C from rivers to the ocean and from the landscape to the atmosphere is especially important in arctic carbon budgets [*McGuire et al.*, 2009], but deeper groundwater contributions to rivers are limited in areas of continuous permafrost [*Kane et al.*, 2003; *Lilly et al.*, 1998; *McNamara et al.*, 1998; *Su et al.*, 2005]. In these areas, groundwater and solutes from the thin, surface thaw layer are delivered to streams. In some large basins like the Yukon River, groundwater comprises less than one quarter of the total river flow, but recent changes in the depth to permafrost have increased groundwater contributions [e.g., *Walvoord and Striegl*, 2007]. These changes in groundwater contribution have both increased and decreased DOC transport to surface waters, resulting in questions about the controls of organic matter export in arctic regions [*Frey and McClelland*, 2009], including what specific hydrologic mechanisms control C export from soils.

In continuous permafrost regions in the low arctic, surface soils are commonly comprised of organic-rich peat, underlain by a layer of mineral soils [e.g., *Walker,* 2000]. Seasonal thawing extends no more than a meter, and results in a shallow but laterally-extensive horizon often saturated with water. Here we collectively refer to any water within the thawed horizon as

'groundwater', and the unconfined aquifer holding it as the 'thawed-layer aquifer' (TLA). Due to large fluctuations of the groundwater table in this TLA, and the substantial role of the groundwater on streamflow after snowmelt [*Quinton and Marsh*, 1999], the TLA has the potential to be an important source of DOC, minerals, and nutrients to surface waters [e.g., *McNamara et al.*, 2008; *Quinton and Pomeroy*, 2006]. However, given the limited depth of this thaw layer, groundwater contributions are often expected to be less important than surface runoff during wet periods. The shallow nature of the TLA combined with a strongly decreasing hydraulic conductivity with depth [*Hinzman et al.*, 1991] creates a unique situation where groundwater contributions are highly dependent on the water table depth [*Quinton and Marsh*, 1999; *Quinton et al.*, 2000], the depth of thaw (ice table depth), and topography [e.g., *Wright et al.*, 2009].

Variability in the water table over short time periods (e.g., hours to days) and throughout a watershed produces hydrologic states ranging from an inundated land surface to a partially drained TLA. When combined with decreasing hydraulic conductivity with depth, these hydrologic states allow for a range of possible mechanisms controlling groundwater flow and solute transport. For example, in addition to shallow groundwater flow within the TLA, exchanges of surface and subsurface water have been suggested in areas of continuous permafrost [*Quinton and Marsh*, 1999; *Quinton and Pomeroy*, 2006], although no specific mechanisms have been proposed or demonstrated. One potential mechanism causing surface-subsurface exchanges is surface topography, operating similarly to bedform-driven hyporheic exchange in rivers where topographic highs produce low pressure zones [*Cardenas and Wilson*, 2007]. In addition, because of high DOC leaching rates from permafrost organic soils [*Judd and Kling*, 2002], surface-subsurface exchanges of water could be an important mechanism controlling carbon transport and influencing DOC concentrations in surface waters.

Here we determine groundwater flow mechanisms in a watershed with continuous permafrost over a range of observed hydrologic conditions, and use numerical groundwater flow simulations to demonstrate the mechanisms and importance of surface-subsurface exchanges across the land surface on carbon transport. A vertically-explicit model to determine micro-

topographic effects and a vertically-integrated model to determine macroscale effects are used to study four scenarios (land surface inundated, land surface with ponded depressions, soil fully saturated, and soil partially-drained) representing the highly variable hydrologic states that occur in these systems. Streamflow data are combined with long-term and synoptic measurements of stream and groundwater DOC concentrations to provide watershed-scale evidence of the role of groundwater in DOC transport and export.

2. Methodology

2.1. The Study Site and Field Observations

Field measurements were made in the first-order Imnavait Creek watershed in the Kuparuk River basin that drains to the Arctic Ocean. Imnavait Creek is located approximately 10 km east of the Toolik Field Station in the northern foothills of the Brooks Range of Alaska. Permafrost is continuous throughout the region and the 2.2 km^2 area above the watershed's main outlet weir (see Site 1 in Figure S1a in the Supporting Information) consists of relatively gentle slopes from hilltop-heath tundra down to a valley bottom of wet-sedge tundra. The hillslopes are covered with moist, acidic tussock tundra and are bisected by "water tracks" that begin just below the ridge, extend into a lower-gradient riparian area, are oriented parallel to the slope and spaced 10-20 m apart, and function to increase hydrologic response time to precipitation events [*McNamara et al.,* 1998, 1999]. Hillslope soils consist of a shallow organic layer (~10-15 cm thick) on top of a mineral soil layer with 10-1000 times lower hydraulic conductivity [*Hinzman et al.*, 1991]. Riparian areas have organic soils up to 1-2 m deep. The TLA develops from completely frozen ground in the spring to thaw depths in late summer that are shallow (20-40 cm) in hillslopes but can approach ~1 m in the riparian areas (see Figure S1b in the Supporting Information). Thaw depths in the study area are representative of tundra on the Alaskan North Slope, where the average end-of-season thaw ranges from 25.5 to 52 cm (data from 1990-2016; [*Circumpolar Active Layer Monitoring Network-CALM, 2017*]).

Stream DOC and flow data were compiled from Site 1 (Supporting Information Figure S1a) for the years spanning 1993-2011 (n=657 samples, Method S1). Water table depths were measured and monitored in the summer of 2015 at ~80 locations throughout a hillslope and riparian zone using temporary and semi-permanent fully-screened piezometers (Supporting Information Figure S1a and c). Pressure transducers were placed in wells (n=12) next to the stream and in the stream (n=6) to monitor water level gradients between the stream and the riparian zone (Supporting Information Figure S1c). The active layer soils were tested for their hydraulic properties using a combination of in-situ slug tests, laboratory analysis of core samples, and previously published work from this site (Supporting Information Method S1). Groundwater samples (n = 255) from the riparian area were also collected and analyzed for DOC (Supporting Information Method S1).

2.2. Numerical Flow Models: Conceptual Basis and Model Description

This investigation of groundwater transport processes considers four scenarios representing the varied hydrologic conditions that can occur throughout highly variable precipitation conditions common in this area and throughout the annual progression of thaw. The scenarios include (1) inundated, (2) ponded, (3) saturated, and (4) partially-drained conditions (Figure 1) where each represents a hydrologic state that happens during the transition from overland flow to the subsequent draining out of the TLA. These conditions can occur due to saturation excess from rain or snowmelt, where overland flow inundates a substantial portion of the land surface (particularly in the flatter riparian areas) when thaw is very shallow early in the season or a smaller portion of the land surface when thaw is deeper (Figure 1a). As the drain out process begins the soils are still saturated and some surface water remains as ponded water in depressions (Figure 1b). This is generally followed by conditions with no surface storage of water, but the subsurface is still saturated (Figure 1c), creating the third scenario more commonly found in flat riparian-zone soils that stay saturated longer than hillslope soils [*Stieglitz et al.*, 2003]. Finally, during periods without additional precipitation, the TLA partially drains and forms a vadose zone and a water table below the land surface (Figure 1d). The varied terrain in these landscapes allows these scenarios to

potentially occur at different locations and times depending on position within the watershed, depth of thaw, antecedent conditions, and precipitation intensity and duration.

Two types of numerical groundwater flow models were used to explore the dominant transport mechanisms: a vertically-explicit (VE) model for scenarios 1-3 to understand the independent role of micro-topography (centimeters to meters scale), and a vertically-integrated (VI) or depth-averaged model for scenario 4 that focused on macroscale processes (100s of meters scale) and provided information regarding catchment-scale responses. The VE model calculates a flow field along a vertical cross-section (*x*-*z* plane) (Supporting Information Method S2), focuses on the conditions in the riparian area, and accounts for micro-topographic influences. The VI model provides a groundwater flow field in the *x*-*y* plane (plan view) (Supporting Information Method S3), considers the entire watershed area, and is forced by macro-topographic gradients.

VE models were constructed for a 20-m section of the low-gradient riparian zone to characterize the connection between the hillslope and stream. To more explicitly link the mechanistic simulations to the potential for DOC production from leaching, groundwater age - the time since a water parcel was infiltrated from an influx boundary (the land surface) - was also calculated for the VE models. Topography was resolved in these models at a 10-cm horizontal resolution from ground-based LiDAR data. The land surface was set as the top boundary of the model domain and a no-flow bottom boundary represents the frozen saturated soils or ice table. The ice table was assumed to have the same shape as the land surface based on strong correlations between the two surfaces measured at different spatial scales (Supporting Information Figure S2). The ice table depths were set to 10 and 30 cm to represent early and mid-season thaw depths (Supporting Information Figure S1b). The three scenarios were modeled with different spatially variable, but steady prescribed head (Dirichlet boundary conditions) at the top (see Figure S3 in the Supporting Information). The inundated model applied a pressure head prescribed from the output of a separate computational fluid dynamics model for the turbulent, inundating overland flow (see Figure S3c and Method S2 in the Supporting information). The saturated model took the surface elevation as the head (h=z). The ponded model is the same as the saturated model, but the water

surface elevation in depressions was set to the immediate local high at the downslope end (i.e., the land surface was 'pit-filled').

Because the VE model represents a vertical cross-section, it requires explicit representation of the vertical variability in hydraulic conductivity (K) and porosity. A power function that represents the decay in saturated K over depth was developed based on in-situ and laboratory measurements (see Method S1 in the Supporting Information) in combination with published values from *Hinzman et al.* [1991]. We used power functions because they typically represent the vertical distribution of the poro-mechanical properties of compacting, consolidating, or cementing porous media [e.g., *Gleeson et al.,* 2016]. K values were translated into permeability (K times the kinematic viscosity divided by the acceleration of gravity or Kv/g) decay with depth (Supplementary Information Figure S3a). A linear function representing the decay of porosity with depth was also estimated based on the reported data from Hinzman et al. [*1991*] (Supplementary Information Figure S3b).

The simpler VI model assumed the water table was a replica of the land surface (Supporting Information Figure S2a, S2b) as derived from a 3-m horizontal resolution DEM. At this resolution, micro-topographic variations are subdued. Local groundwater flow rates and directions were calculated using the land surface slope as the hydraulic gradient and an imposed aquifer transmissivity. We determined transmissivity by assuming different values for homogeneous hydraulic conductivity and saturated thickness that represented average conditions across the study site (see Supporting Information Method S3 for details). The VI model was implemented for the entire watershed upstream of Site 1 (Figure S1a). However, we also focused on a 600 m × 300 m portion of the watershed where detailed water table mapping was completed to verify modeling results (Figure S4c). Under partially drained conditions, all river flow is sustained by groundwater flow, i.e., baseflow. Thus, we again determined the validity of the VI modeling approach for a time when detailed saturated thickness measurements were used to parameterize the VI model. The VI model groundwater fluxes to the stream accumulated from the area contributing to the weirs ($Q_{gw,VI}$) were compared to in-stream volumetric discharge values during baseflow conditions ($Q_{gw,W}$)

(see Method S4 in the Supporting Information). Finally, the VI model-based estimates of baseflow were compared to the groundwater flux estimates into the stream along a 100-m reach from head gradients based on near-stream wells and stream water surface elevations. Using Darcy's law and a vertical average of measured hydraulic conductivities, the cumulative groundwater flux ($Q_{gw,D}$) was calculated for the 100-m long reach. These fluxes were then extrapolated to the entire contributing area to provide an estimate of the total volume from the watershed and then compared to the VI model ($Q_{gw,VI}$) and weir ($Q_{gw,W}$) estimates (see Method S4 for details).

3. Results and Discussion

3.1. Modeled Groundwater Flow Fields and Exchanges

The inundated scenario shows repeated exchanges of the overland flow water with the groundwater. These exchanges are driven by pressure differences induced by micro-topography (Figure 2a and Table S1; the pressure profiles along the land surface are presented in Figure S5 in the Supporting Information). The mechanism in this exchange is the same as bedform-driven hyporheic exchange where topographic highs (flow constrictions due to shallower flow depth) accelerate turbulent open channel flow and produce low pressure zones [*Cardenas and Wilson*, 2007]. On land, this mechanism causes exchanges or "porpoising" of water from above to below the land surface moving downslope. As shown by the flow paths (lines) and directions (arrows) (Figure 2A), the entire depth of the TLA is influenced by the exchanges from the surface, and the exchange flow cells (or portions of the TLA where water enters the subsurface and then returns to the surface further down gradient) are interrupted by relatively larger topographic features. This is also analogous to bedforms in rivers defining isolated hyporheic exchange flow cells [*Cardenas and Wilson*, 2007].

We quantify the relevance of these exchanges with the ratio of total groundwater flux across the land surface (top boundary of the groundwater flow model domain) divided by the overland flow flux (Supporting Information Table S1). Because the groundwater exchange increases with the velocity of the surface water, just as in riverbed hyporheic flow mechanics [*Cardenas and*

Wilson, 2007], this flux ratio is a function of surface flow velocity. It is clear that the overland flow water exchanges with the subsurface many times when traveling towards the stream. For example, depending on the mean overland flow velocities we imposed as boundary conditions (0.01 m s^{-1} to 0.25 m s^{-1}), from 4 to 68% of the groundwater is exchanged with overland water specifically over the 20-m long model domain (Supporting Information Table S1). To generalize, the ratio can be expressed per meter length (downslope) of landscape, and using this information the turnover length can be calculated – this is the cumulative length it takes for the ratio to reach unity. The turnover length was found to range from 30-570 m. The hillslope-riparian zone of Imnavait Creek is around 600 m, and many hillslopes and riparian zones are much broader than this in this area. Contiguous overland flow across the entire hillslope-riparian zone of Imnavait Creek is unlikely, except within water tracks during the wettest of conditions and during times of limited thaw. However, inundated areas spanning several meters to a few tens of meters are realistic throughout much of the watershed, particularly in flatter riparian areas, and are observed during times of limited thaw, substantial snowmelt, or intense rain events [e.g., *Kane et al.*, 2003]. This bulk analysis also ignores the details of the flow paths, because the calculations assume that each exchange is between that of well-mixed boxes (which is not the case). Thus, the calculation is an indicator of the average extent of the exchange because some water parcels may be exchanged many more times than this ratio while others may never enter the subsurface.

The VE models for the ponded case produced a sequence of flow cells with flow originating from either an upslope topographic high or an upslope ponded depression and ending at the next downslope depression (Figure 2b). The ponds have a groundwater discharge zone in the upslope half and groundwater recharge locations in the downslope half. This mechanism is identical to a series of groundwater flow-through lakes [*Townley,* 2000*; Winter,* 1995]. When the ice table was shallow, the TLA had insufficient depth to allow for the longer flow paths to develop, and instead very local circulation cells were created beneath the ponds with discharge and recharge focused only at the edges of the ponds. The groundwater exchange rates (or groundwater efflux) during ponded conditions are of the same magnitude but smaller when compared to the exchange rates

for the inundated models (Table S1). The overall exchange fluxes were relatively unaffected by the depth of the bottom boundary ice table.

The VE models representing fully saturated conditions (but not inundated nor ponded) show that micro-topography is causing groundwater to be cycled toward the surface and back through the subsurface repeatedly (Figure 2c). The flow fields are a downscaled version of topography-driven regional groundwater flow where the water table mimics topography (i.e., the mechanism is the same as Tóthian regional groundwater flow [*Cardenas and Jiang*, 2010; *Tóth*, 1963]). In this situation, groundwater infiltrates in topographic highs and exfiltrates in depressions. The local groundwater head gradients driven by micro-topography are also much larger than the macro-topographic slope (the general inclination of the hillslope-riparian zone towards Imnavait Creek), leading to isolated circulation cells of groundwater. The exchange rates of the saturated models were larger than in the ponded models (Supporting Information Table S1) because the micro-topography leads to large local head gradients that are limited within ponds that submerge a portion of the topography. Despite representing different mechanisms that lead to some differences in flow magnitude (Figure 2), all the VE models above – inundated, ponded, saturated – suggest that local topography and the depth distribution of *K* produce the substantial exchange across the land surface for groundwater over a range of thaw depths.

When the water table is below the land surface during partially-drained conditions, both the field measurements (Supporting Information Figure S2) and models show that macro-topography is the dominant control on groundwater flow (Supporting Information Figure S4). The VI modeled discharge for partially-drained conditions is similar to measured streamflow (Table S2). However, the model estimates, which use an average *K* and measured saturated thickness, were consistently lower because they did not explicitly account for the contributions from the topmost zone of the aquifer with the highest *K* or permeability (Figure S3a). That is, in some areas in the watershed, if the water table was near the land surface, flows occurring in the shallower, higher hydraulic conductivity layers would not be accounted for in the VI model. It is also likely that other preferential subsurface flow paths could exist [*Wright et al.*, 2009] that would be missed due to the

assumed homogeneity in the model. It is therefore not surprising that the VI model under-predicts stream discharge during baseflow conditions, while still providing reasonable estimates of groundwater contributions. The direct Darcy flux estimates ($Q_{gw,D}$) were in between the model and the weir estimates, larger than $Q_{gw,VI}$, but still less than $Q_{gw,W}$ (Table S2). The different comparisons suggest that the VI model driven by macro-topography provides reasonable (but potentially low) estimates of groundwater contributions when the TLAs are partially drained.

3.2. Integrated Watershed Observations and Synthesis: Hydrographs and Chemographs

The models for the four scenarios all point to groundwater flows and exchanges being an important transport mechanism for solutes across the range of hydrologic states. Based on the modeling results above, in Imnavait Creek, or in any other watershed with similar vertical variability in *K*, it is expected that stream flow is primarily comprised of groundwater or of water influenced by overland flow that was intermittently groundwater. This surface-subsurface exchange coupled with high leaching rates of DOC should translate into stream water with very similar chemistry to water flowing through the TLA if in-stream processing of DOC is limited.

As our models and mechanisms of rapid surface-subsurface exchange would predict, stream water DOC concentrations were consistently similar to those in groundwater within the TLA soil (n=255, Figure 3, Figure S6 in Supporting Information). During low discharge, when flow is dominated by groundwater input, some stream concentrations approached and dropped below minimum observed groundwater concentrations. This can be explained in part by longer water residence times within the stream that would result in greater DOC processing and removal, for example by bacterial respiration or photo-mineralization of DOC in surface water [*Cory et al.*, 2014, 2015]. In contrast, during precipitation events or snowmelt the thin TLA can quickly saturate and result in overland flow. Due to low DOC concentrations in precipitation and overland flow, one might expect a dilution of stream water concentrations [*Boyer et al.,* 1999]. However, no such dilution was observed in Imnavait Creek. Stream DOC concentrations were near groundwater concentration ranges during high flow periods with the exception of the end of the freshet (Figure

3) when there was limited thaw. Others have established that stream DOC concentrations during precipitation events or snowmelt depend on source areas, flowpaths, and the rate at which the available DOC is flushed [e.g., *Hornberger et al.*, 1994]. These lower concentrations could be due to a limited DOC pool during this time or dilution due to the extent of overland flow. However, we generally found that during wetter hydrologic states and higher flow, the stream DOC concentrations were most similar to groundwater concentrations (Figure 3). Overall, while the observed variations in DOC concentration with discharge in Imnavait Creek may be related to dilution, to "reaction limitation" in the leaching of peat, or to differential sourcing of groundwater from soils to streams, the results still strongly suggest that groundwater flow and surface-subsurface exchange mechanisms are controlling instream chemistry over a large range of thaw depths, hydrologic conditions, and instream flows. This relative chemostasis in a headwater basin appears to be in contrast with concentration-discharge trends in temperate headwater basins [*Creed et al.*, 2015].

3.3. Groundwater Age and the Production of Dissolved Organic Carbon

For vertical exchanges of overland flow and groundwater to strongly affect DOC concentrations, there must be sufficient leaching rates and contact time with soil organic matter in both shallow and deeper soils. In the soils near Imnavait the production of DOC from organic matter leaching varies from 8.25 to 32.7 μg C per g soil per day [*Judd and Kling*, 2002]. Assuming a typical dry soil bulk density of 0.114 g cm^{-3} and a porosity of 0.85 for the topmost 10 cm of organic matter [ARC LTER, 2017], leaching could produce a concentration of 1.1 - 4.4 mg C L^{-1} for day-old groundwater. Considering that bulk densities for deeper peat soil can be as high as 0.25 g cm^{-3}, day-old groundwater DOC concentrations could range from 2.9 - 11.7 mg C L^{-1}, illustrating higher potential for production in deeper peat layers with higher bulk densities and lower porosity. Consistent with these calculations, observed DOC concentrations in groundwater increased with depth (Table S3). Using the measured soil porosity (and corresponding bulk density) at 20 cm depth

(Figure S3), DOC concentrations after one day of leaching would range from 6.3 - 24.9 mg C L^{-1}, which are similar to observations throughout the riparian area (Figure S6).

The inundated, ponded, and saturated cases show an increased length of time spent within the subsurface, or groundwater age, with depth (Figure 2). The vertical exchange and age distributions suggest that the surface-subsurface exchange mechanism also increases the contribution of relatively deeper, older groundwater from the TLA to the streams via surface runoff containing a mixture of groundwater sourced from varied depths. When thaw depth is shallow, the TLA hosts mostly young groundwater with ages on the order of minutes to hours, but this may still approach a day in the relatively deeper areas, especially under ponds. Groundwater ages easily surpass a day when thaw depth is at 30 cm (Figure 2). Groundwater with ages even less than one day are expected to have high DOC concentrations due to frequent exchange across the land surface and the rapid leaching mentioned above. This means that the older groundwater will have higher concentrations due to increased contact time for DOC production, as illustrated by measured increases in DOC concentration with depth (Table S3). Thus, the modeled age fields for the three states represented by the VE models suggest sufficient contact time between groundwater and the organic matter-rich TLA soils to produce the measured groundwater DOC concentrations (Figure S6, Table S3).

4. Summary and Conclusions

We investigated the poorly known mechanisms of shallow groundwater flow and exchanges across the land surface in the thawed layer of a first-order arctic watershed using numerical groundwater flow models. The vertically explicit models represented hydrologic states when the thawed layer aquifer above the continuous permafrost (1) was inundated by overland flow, (2) land-surface depressions were ponded by water, (3) the land surface was at saturation, or (4) the thawed layer was partially drained. Detailed field and laboratory measurements from Imnavait Creek guided model parameterization. The mechanisms for each hydrologic state, although different, all suggested high rates of groundwater flow and exchanges across the land surface

during transport to the stream due to micro-topography, sufficiently permeable soils, and decreasing hydraulic conductivity with depth. Direct and watershed-scale calculations of groundwater flow contributions to the stream corroborate the vertically integrated flow model estimates, and further suggest substantial groundwater contributions during partially drained conditions. For the three wetter conditions, minimum groundwater ages within the thawed layer spanned minutes to days, which is sufficient for the high leaching rates of carbon from the soil organic matter to produce the measured high concentrations of groundwater DOC. Groundwater samples taken along a transect of the riparian zone showed variable but generally high DOC concentrations. Contributions of this consistently high DOC groundwater to Imnavait Creek resulted in low variability in stream concentrations (relative chemostasis) throughout a period spanning close to two decades and representing six orders of magnitude in streamflow. The models and integrated hydrologic and chemical observations all support the consistent importance of groundwater flow and exchanges of water and dissolved organic carbon across the land surface that influence instream chemistry. We propose that the flow and exchange mechanisms illustrated here will occur in basins of all sizes and locations given adequate micro-topography, sufficient permeability of surface soils, and decreasing hydraulic conductivity with depth. Such advances in understanding groundwater flow and transport mechanisms are needed given that thawing permafrost will result in deeper, carbon-rich thaw layer aquifers that can further increase carbon export from the landscape.

Acknowledgements

We thank Douglas Kane, Rose Cory, Levi Overbeck, Jason Dobkowski, Christopher Cook, Matthew Kaufman, Kevin Befus, Peter Zamora, Gauis Shaver, Anne Giblin, and scientists at the Toolik Lake Arctic LTER and Toolik Lake Field Station (GIS, R. Fulweber, J. Stuckey) for assistance or advice. This research was supported in part by NSF grants OPP 1204220, 1023270, 1022876; ARC 1107707,

1504006; PLR 1107593, 1504006; and DEB 1026843, 1147378, 1347042, 1637459. M.B.C. and M.T.O were partly supported by the Geology Foundation at The University of Texas at Austin and by student grants from the Geological Society of America and the American Association of Petroleum Geologists.

Data analyzed within the study are publicly available at http://arc-lter.ecosystems.mbl.edu/data-catalog, http://ine.uaf.edu/werc/projects/NorthSlope/imnavait/flume/flume.html, and the remainder is currently available at https://usu.box.com/s/1wxlm88y4w3pxzc96nmtilq0bwn4wpws and will be archived via https://www.hydroshare.org/ once the paper is accepted.

References

Alexander, R. B., E. W. Boyer, R. A. Smith, G. E. Schwarz, and R. B. Moore (2007), The Role of Headwater Streams in Downstream Water Quality, JAWRA Journal of the American Water Resources Association, 43(1), 41-59.

Arctic Long Term Ecological Research (ARC LTER) Data Archives (2017). at < http://arc-lter.ecosystems.mbl.edu/terrestrial-data>

Boyer, E.B., Hornberger, G.M., Bencala, K.E., and D.M. McKnight (1997), Response characteristics of DOC flushing into an alpine catchment stream, Hydrological Processes, 11(12), 1635-1647.

Circumpolar Active Layer Monitoring Network-CALM: *Long-Term Observations of the Climate-Active Layer-Permafrost System* (2017). at < *https://www2.gwu.edu/~calm/data/north.html* >

Cardenas, M. B., and J. L. Wilson (2007), Dunes, turbulent eddies, and interfacial exchange with permeable sediments, Water Resources Research, 43(8).

Cardenas, M. B., and X.-W. Jiang (2010), Groundwater flow, transport, and residence times through topography-driven basins with exponentially decreasing permeability and porosity, Water Resources Research, 46(11).

Cory, R. M., C. P. Ward, B. C. Crump, and G. W. Kling (2014), Sunlight controls water column processing of carbon in arctic fresh waters, Science, 345(6199), 925-928.

Cory, R. M., K. H. Harrold, B. T. Neilson, and G. W. Kling (2015), Controls on dissolved organic matter (DOM) degradation in a headwater stream: the influence of photochemical and hydrological conditions in determining light-limitation or substrate-limitation of photo-degradation, Biogeosciences, 12(22), 6669-6685.

Creed, I. F., et al. (2015), The river as a chemostat: fresh perspectives on dissolved organic matter flowing down the river continuum, Canadian Journal of Fisheries and Aquatic Sciences, 72(8), 1272-1285.

Dhillon, G. S., and S. Inamdar (2014), Storm event patterns of particulate organic carbon (POC) for large storms and differences with dissolved organic carbon (DOC), Biogeochemistry, 118(1), 61-81.

Frey, K. E., and J. W. McClelland (2009), Impacts of permafrost degradation on arctic river biogeochemistry, Hydrological Processes, 23(1), 169-182.

Gleeson, T., K. M. Befus, E. Luijendijk, S. Jasechko, and M. B. Cardenas (2016), The global volume and distribution of modern groundwater, Nature Geoscience, 9, 161–167.

Hinzman, L. D., D. L. Kane, R. E. Gieck, and K. R. Everett (1991), Hydrologic and thermal properties of the active layer in the Alaskan Arctic, Cold Regions Science and Technology, 19(2), 95-110.

Hornberger, G.M., Bencala, K.E. and D.M. McKnight (1994), Hydrological controls on the temporal variation of dissolved organic carbon in the Snake River near Montezuma, Colorado. Biogeochemistry, 25, 147-165.

Jencso, K. G., B. L. McGlynn, M. N. Gooseff, S. M. Wondzell, K. E. Bencala, and L. A. Marshall (2009), Hydrologic connectivity between landscapes and streams: Transferring reach- and plot-scale understanding to the catchment scale, Water Resources Research, 45(4).

Judd, K. E., and G. W. Kling (2002), Production and export of dissolved C in arctic tundra mesocosms: the roles of vegetation and water flow, Biogeochemistry, 60(3), 213-234.

Kane, D. L., J. P. McNamara, D. Yang, P. Q. Olsson, and R. E. Gieck (2003), An Extreme Rainfall/Runoff Event in Arctic Alaska, Journal of Hydrometeorology, 4(6), 1220-1228.

Lilly, E. K., D. L. Kane, L. D. Hinzman, and R. E. Gieck (1998), Annual water balance for three nested watersheds on the North Slope of Alaska, Arctic F orum, 53.

McGlynn, B. L., and J. J. McDonnell (2003), Role of discrete landscape units in controlling catchment dissolved organic carbon dynamics, Water Resources Research, 39(4).

McGuire, A. D., L. G. Anderson, T. R. Christensen, S. Dallimore, L. Guo, D. J. Hayes, M. Heimann, T. D. Lorenson, R. W. Macdonald, and N. Roulet (2009), Sensitivity of the carbon cycle in the Arctic to climate change, Ecological Monographs, 79(4), 523-555.

McNamara, J. P., D. L. Kane, and L. D. Hinzman (1998), An analysis of streamflow hydrology in the Kuparuk River Basin, Arctic Alaska: a nested watershed approach, Journal of Hydrology, 206(1), 39-57.

McNamara, J. P., D. L. Kane, and L. D. Hinzman (1999), An analysis of an arctic channel network using a digital elevation model, Geomorphology, 29(3-4), 339-353.

McNamara, J. P., D. L. Kane, J. E. Hobbie, and G. W. Kling (2008), Hydrologic and biogeochemical controls on the spatial and temporal patterns of nitrogen and phosphorus in the Kuparuk River, arctic Alaska, Hydrological Processes, 22(17), 3294-3309.

Quinton, W. L., and P. Marsh (1999), A conceptual framework for runoff generation in a permafrost environment, Hydrological Processes, 13(16), 2563-2581.

Quinton, W. L., and J. W. Pomeroy (2006), Transformations of runoff chemistry in the Arctic tundra, Northwest Territories, Canada, Hydrological Processes, 20(14), 2901-2919.

Quinton, W. L., D. M. Gray, and P. Marsh (2000), Subsurface drainage from hummock-covered hillslopes in the Arctic tundra, Journal of Hydrology, 237(1), 113-125.

Stieglitz, M., J. Shaman, J. McNamara, V. Engel, J. Shanley, and G. W. Kling (2003), An approach to understanding hydrologic connectivity on the hillslope and the implications for nutrient transport, Global Biogeochem. Cycles, 17 (4), 1105.

Su, F., J. C. Adam, L. C. Bowling, and D. P. Lettenmaier (2005), Streamflow simulations of the terrestrial Arctic domain, Journal of Geophysical Research: Atmospheres, 110(D8).

Tóth, J. (1963), A theoretical analysis of groundwater flow in small drainage basins, Journal of Geophysical Research, 68(16), 4795-4812.

Townley, L. R., and M. G. Trefry (2000), Surface water-groundwater interaction near shallow circular lakes: Flow geometry in three dimensions, Water Resources Research, 36(4), 935-948.

Wagener, T., M. Sivapalan, P. Troch, and R. Woods (2007), Catchment Classification and Hydrologic Similarity, Geography Compass, 1(4), 901-931.

Walker, D. A. (2000), Hierarchical subdivision of Arctic tundra based on vegetation response to climate, parent material and topography, Global Change Biology, 6, 19-34.

Walvoord, M. A., and R. G. Striegl (2007), Increased groundwater to stream discharge from permafrost thawing in the Yukon River basin: Potential impacts on lateral export of carbon and nitrogen, Geophysical Research Letters, 34(12).

Winter, T. C., and D. O. Rosenberry (1995), The interaction of ground water with prairie pothole wetlands in the Cottonwood Lake area, east-central North Dakota, 1979–1990, Wetlands, 15(3), 193-211.

Wright, N., M. Hayashi, and W. L. Quinton (2009), Spatial and temporal variations in active layer thawing and their implication on runoff generation in peat-covered permafrost terrain, Water Resources Research, 45(5).

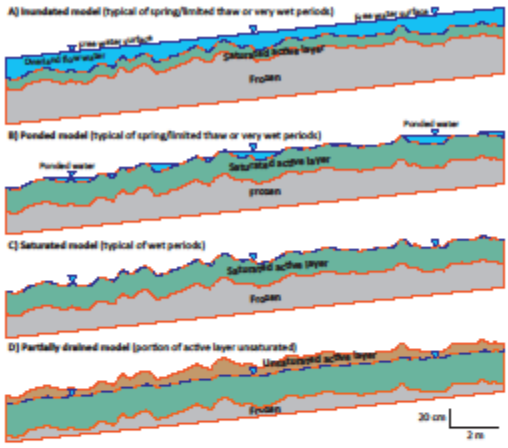

Fig. 1. Conceptual models guiding the analysis and modeling of groundwater flow mechanisms in thawed active layer aquifers. The four models represent different hydrologic and thaw depth conditions.

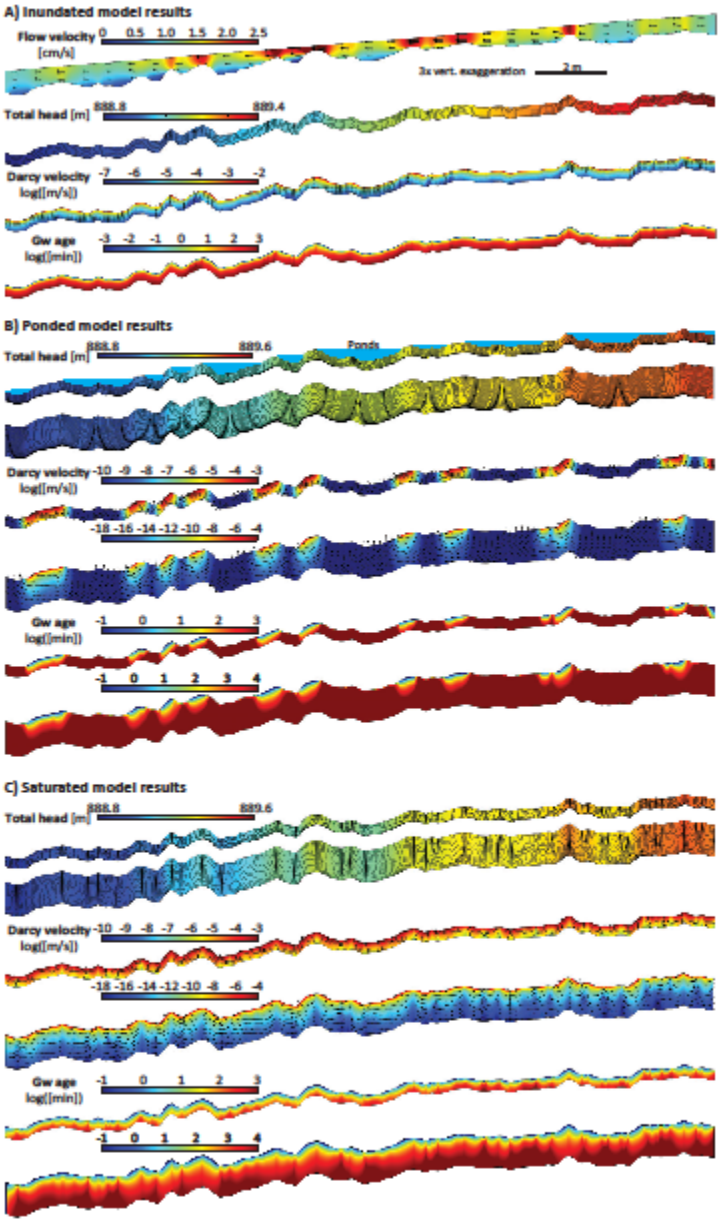

Fig. 2. Groundwater head, flow, and age fields resulting from vertically-explicit modeling of inundated, ponded, and saturated conditions. The solid lines are flowlines whereas the arrows indicate flow direction and not magnitude. The inundated model (A) also shows a modeled overland flow field whose pressure output drives the groundwater flow model. Results for the ponded (B) and saturated conditions (C) at two thaw depths (10 cm and 30 cm) are shown. The color scale for the age field is truncated and there are ages at depth that go beyond the maximum.

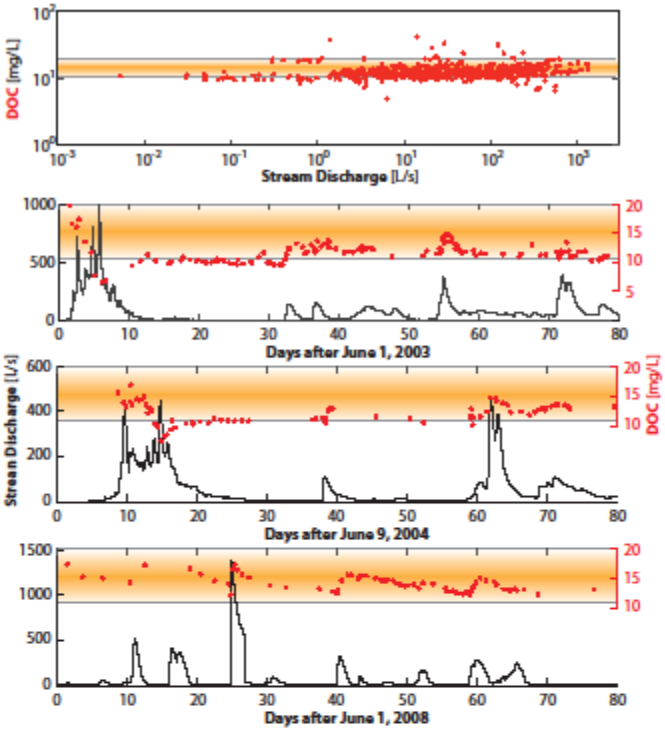

Fig. 3. The top panel shows all stream DOC concentration (C) data (from Site 1, years 1993-2011, n=657) plotted against discharge (Q); the linear, low-slope relationship between C and Q illustrates relative chemostasis. The orange shading represents the range of DOC concentrations in groundwater (n=255) sampled 10-40 m away from the stream (Figure S6), with the darkest color representing the mean concentration and the dashed lines representing ± one standard deviation. The bottom three panels show representative hydrographs and DOC chemographs at Site 1 (Figure S1, S4) in three summers of differing discharge (black curve). Orange shading illustrating groundwater DOC concentrations is the same as for the top panel.